BRAIN
ORIGINAL ARTICLE

C-terminal TMEM106B fragments in human brain correlate with disease-associated *TMEM106B* haplotypes

Cristina T. Vicente,[1,2,†] Jolien Perneel,[1,2,†] Sarah Wynants,[1,2] Bavo Heeman,[1,2] Marleen Van den Broeck,[1,2] Matt Baker,[3] Simon Cheung,[4] Júlia Faura,[1,2] Ian R. A. Mackenzie[4,5] and Rosa Rademakers[1,2,3]

[†]These authors contributed equally to this work.

Transmembrane protein 106B (TMEM106B) is a tightly regulated glycoprotein predominantly localized to endosomes and lysosomes. Genetic studies have implicated *TMEM106B* haplotypes in the development of multiple neurodegenerative diseases with the strongest effect in frontotemporal lobar degeneration with TDP-43 pathology (FTLD-TDP), especially in progranulin (*GRN*) mutation carriers.

Recently, cryo-electron microscopy studies showed that a C-terminal fragment (CTF) of TMEM106B (amino acid residues 120–254) forms amyloid fibrils in the brain of patients with FTLD-TDP, but also in brains with other neurodegenerative conditions and normal ageing brain. The functional implication of these fibrils and their relationship to the disease-associated *TMEM106B* haplotype remain unknown.

We performed immunoblotting using a newly developed antibody to detect TMEM106B CTFs in the sarkosyl-insoluble fraction of post-mortem human brain tissue from patients with different proteinopathies ($n = 64$) as well as neuropathologically normal individuals ($n = 10$) and correlated the results with age and *TMEM106B* haplotype. We further compared the immunoblot results with immunohistochemical analyses performed in the same study population.

Immunoblot analysis showed the expected ~30 kDa band in the sarkosyl-insoluble fraction of frontal cortex tissue in at least some individuals with each of the conditions evaluated. Most patients with *GRN* mutations showed an intense band representing TMEM106B CTF, whereas in most neurologically normal individuals it was absent or much weaker. In the overall cohort, the presence of TMEM106B CTFs correlated strongly with both age ($r_s = 0.539$, $P < 0.001$) and the presence of the *TMEM106B* risk haplotype ($r_s = 0.469$, $P < 0.001$). Although there was a strong overall correlation between the results of immunoblot and immunohistochemistry ($r_s = 0.662$, $P < 0.001$), 27 cases (37%) were found to have higher amounts of TMEM106B CTFs detected by immunohistochemistry, including most of the older individuals who were neuropathologically normal and individuals who carried two protective *TMEM106B* haplotypes.

Our findings suggest that the formation of sarkosyl-insoluble TMEM106B CTFs is an age-related feature which is modified by *TMEM106B* haplotype, potentially underlying its disease-modifying effect. The discrepancies between immunoblot and immunohistochemistry in detecting TMEM106B pathology suggests the existence of multiple species of TMEM106B CTFs with possible biological relevance and disease implications.

1 VIB Center for Molecular Neurology, University of Antwerp, 2610, Antwerp, Belgium
2 Department of Biomedical Sciences, University of Antwerp, 2610, Antwerp, Belgium
3 Department of Neuroscience, Mayo Clinic, Jacksonville, FL 32233, USA
4 Department of Pathology, Vancouver Coastal Health, Vancouver, BC V5Z1M9, Canada
5 Department of Pathology, University of British Columbia, Vancouver, BC V6T 1Z7, Canada

Received December 13, 2022. Revised March 03, 2023. Accepted April 13, 2023. Advance access publication April 26, 2023

Correspondence to: Rosa Rademakers, PhD
VIB Center for Molecular Neurology, Universiteitsplein 1, 2610 Wilrijk, Belgium
E-mail: rosa.rademakers@uantwerpen.vib.be

Correspondence may also be addressed to: Ian R. A. Mackenzie, MD, FRCPC
Department of Pathology, University of British Columbia
2211 Wesbrook Mall, Vancouver, BC V6T 2B5, Canada
E-mail: Ian.mackenzie@vch.ca

Keywords: TMEM106B; neurodegeneration; haplotype; progranulin; fibrils

Introduction

Recent cryo-electron microscopy (cryo-EM) studies found that a C-terminal fragment (CTF) [amino acid residues (AA) 120–254] of transmembrane protein 106B (TMEM106B) can form amyloid filaments in the brain of patients with frontotemporal lobar degeneration (FTLD) with TAR DNA-binding protein 43 (TDP-43) pathology (FTLD-TDP) as well as other neurodegenerative disorders and in the normal ageing brain.[1–4] The accumulation of filamentous protein aggregates is a hallmark of most neurodegenerative disorders, with inclusions of tau, amyloid-β (Aβ), α-synuclein and TDP-43 being recognized as important drivers of disease.[5,6] However, the pathogenicity and disease contribution of TMEM106B filaments is not immediately apparent as they were also identified in the normal ageing brain and in multiple neurodegenerative disorders, characterized by the accumulation of other aggregating proteins.

TMEM106B is a single-pass, type II transmembrane protein localized in the membrane of late endolysosomal compartments, where it plays an important role in lysosomal function and regulates lysosomal morphology, trafficking and maturation.[7–10] The C-terminus resides within the lysosomal lumen and is highly glycosylated, with five glycosylation motifs at N145, N151, N164, N183 and N256.[11] While the precise mechanism is unknown, TMEM106B can be proteolytically processed and releases its C-terminal domain in the lysosomal lumen, which is presumably a prerequisite for the formation of TMEM106B filaments.[12]

Interestingly, genetic variants in *TMEM106B* have been associated with the risk of developing disease for most of the neurodegenerative disorders in which TMEM106B fibrils were originally identified.[13,14] *TMEM106B* was first identified as a genetic risk factor for FTLD-TDP in 2010.[15] FTLD is the second most common dementia in people under the age of 65 years and represents 10–20% of all dementias with an early disease onset.[16,17] Approximately half of all FTLD cases are characterized by the accumulation of TDP-43 and can be classified as pathology subtypes A through E, based on the morphology and distribution of the TDP-43 inclusions.[18,19] The disease-modulating effect of *TMEM106B* was found to be especially prominent in FTLD-TDP patients with heterozygous loss-of-function mutations in the progranulin (*GRN*) gene but was later also replicated in FTLD-TDP patients carrying the *C9orf72* hexanucleotide GGGGCC repeat expansion.[20,21] In addition, *TMEM106B* has been linked to healthy ageing phenotypes where it may provide neuronal protection against age-related degeneration.[22,23] In all these studies, a set of single nucleotide polymorphisms (SNPs) in high linkage disequilibrium with each other in the genomic region of *TMEM106B* were found to be associated with the respective phenotypes, making it impossible to determine the functional variant(s) responsible for modulating disease risk. Consequently, the associated variants are collectively combined into a risk and a protective *TMEM106B* haplotype. The only coding variant that differentiates the two haplotypes (threonine to serine change at amino acid position 185) is often used as denominator to represent the haplotypes; however, functional effects of non-coding variants on the haplotype have also been reported.[24] While the mechanism by which *TMEM106B* haplotypes influence neurodegenerative disease and ageing is not known, accumulating evidence suggests it may relate to TMEM106B levels.[24,25] The functional implication of TMEM106B fibrils and their possible relationship to the disease-associated *TMEM106B* haplotypes however have not previously been assessed.

To address this knowledge gap, we used a newly developed antibody against a C-terminal epitope of TMEM106B to perform immunoblotting and immunohistochemistry (IHC) on post-mortem human brain tissue of patients with FTLD-TDP, other neurodegenerative conditions and normal ageing. We found that the formation of sarkosyl-insoluble TMEM106B CTFs is an age-related feature of neurodegenerative diseases which is strongly modified by *TMEM106B* haplotype, with higher levels of CTFs in the risk haplotype carriers, potentially underlying its disease-modifying effect.

Materials and methods

Study population and cohort selection

The post-mortem material used in this study was provided by the University of British Columbia Clinic for Alzheimer's Disease and Related Disorders (CARD). All patients were evaluated at CARD and provided consent to participate in research studies in accordance with the Declaration of Helsinki and local ethics review board standards. Fixed and frozen tissue from both frontal cortex and cerebellum were available for research. The laterality of the hemisphere from which each type of specimen was obtained had not been recorded at the time of sampling and was not systematically assessed. The neuropathological evaluation was performed according to standard guidelines for the assessment of dementia.[26] The FTLD-TDP cases were classified into pathological subgroups according to current pathological criteria.[19]

For this study, we selected autopsy cases with different proteinopathies ($n = 64$) as well as neuropathologically normal individuals ($n = 10$) with a broad age range within each group. We specifically aimed to include cases carrying different copy numbers of the *TMEM106B* risk/protective haplotype. Cases were further selected based on their pathological diagnosis, including (i) different subtypes of FTLD-TDP of both genetic [*GRN* mutation carriers, ($n = 10$) and *C9orf72* expansion carriers ($n = 5$ with type A, $n = 4$ with type B)] and sporadic [type A ($n = 4$), type B ($n = 8$), and type C ($n = 9$)] origin; (ii) Alzheimer's disease ($n = 8$); (iii) Lewy body disease

(diffuse LBD, $n = 7$) and multiple system atrophy ($n = 2$) to represent synucleinopathies; and (iv) corticobasal degeneration ($n = 2$) and progressive supranuclear palsy ($n = 5$) to represent primary tauopathies. No significant differences were observed among the pathological subgroups within the study population with regards to sex ($P = 0.738$) or age ($P = 0.336$). Detailed information on all human donors is provided in Supplementary Table 1.

Genotyping

Genomic DNA was extracted from post-mortem brain tissue using the QiAmp DNA Mini kit (Qiagen, 51304) following the manufacturer's protocol. Genotyping was performed according to standard procedures by amplification of PCR fragments followed by Sanger sequencing of *TMEM106B* SNPs rs1990622 (C>T, non-coding sentinel SNP) and rs3173615 (C>G, encoding p.T185S) and *GRN* SNP rs5848 (C>T, SNP in 3′ untranslated region reported to affect disease risk in several conditions). For all samples included in the study, *TMEM106B* SNPs rs1990622 and rs3173615 were found to be in complete linkage disequilibrium. As such, statistical analyses were performed only with *TMEM106B* haplotypes, where the C-allele of rs3173615 (corresponding to a threonine at AA185) denotes the risk haplotype.

Antibody generation

We generated a rabbit polyclonal antibody raised against a synthetic peptide corresponding to C-terminal AA239–250 of human TMEM106B, located within the filament-forming fragment.[1–4] Peptide production, immunization, and immunopurification was performed by Eurogentec (Belgium). The antibody is hereafter referred to as VIB_SB0051.

Immunoblot analyses

Protein fractionation of post-mortem human brain samples

Frontal cortex and cerebellum tissues (100 mg) were homogenized in cold buffer A (10 mM Tris-HCl pH 7.4, 80 mM NaCl, 1 mM $MgCl_2$, 1 mM EGTA, 0.1 mM EDTA, phosphatase and protease inhibitors) using an Ultra-Turrax tissue homogenizer (±20 s, speed 5) and further disrupted by passing the homogenate through a sterile 21G needle for a minimum of 10 times or until fully homogeneous. The homogenates were spun at 150 000*g* for 70 min at 4°C [Beckman Optima Max XP tabletop ultracentrifuge, TLA-110 (all samples) or TLA-100 (subset of samples) rotors]. The resulting supernatant (S1) was kept aside and the pellet (P1) was resuspended in cold buffer B (10 mM Tris HCl pH 7.4, 850 mM NaCl, 1 mM EGTA, and 10% sucrose). Samples were then centrifuged at 14 000*g* for 10 min at 4°C to remove any remaining large debris. The pellet (P2) was kept aside while the supernatant (S2) was adjusted to 1% sarkosyl and kept shaking for 1 h at room temperature. The samples were then centrifuged at 150 000*g* for 40 min at 4°C to result in a sarkosyl-soluble supernatant (S3) and sarkosyl-insoluble pellet (P3) (schematically represented in Fig. 1A).

For the determination of full-length TMEM106B in a standard RIPA-soluble fraction, 30 µl of the tissue homogenate was incubated in an equal volume of ice-cold 2× RIPA (50 mM Tris-HCl pH 7.5, 300 mM NaCl, 2% NP-40, 1% sodium deoxycholate, 0.2% SDS, phosphatase and protease inhibitors) and lysed on ice for 30 min, with a short vortex every 5 min. The lysate was centrifuged at 14 000*g* for 20 min at 4°C and the supernatant was kept as the RIPA-soluble (RIPAsol) fraction.

Immunoblotting

Sarkosyl-insoluble pellets (P3) were resuspended in PBS, agitated overnight at 4°C and sonicated at 45 kHz for 10 min in ice water (sonicator bath 142-6046, VWR). The S1 fractions and sarkosyl-soluble fractions (S3) were concentrated using Vivaspin500 columns (Sigma-Aldrich, Z614009-25EA). The extracts were diluted in NuPAGE LDS sample buffer (Invitrogen, NP0007) supplemented with 5% β-mercaptoethanol (Sigma-Aldrich, M6250) and further denatured by boiling for up to 5 min at 95°C. Electrophoresis was performed using NuPAGE Novex 12% Bis-Tris Gels (Invitrogen, NP0341) in NuPAGE MOPS SDS running buffer (Invitrogen, NP0001). Fractions were loaded volumetrically. For the determination of full-length TMEM106B levels, the concentration of RIPA-soluble protein extracts was measured using the Pierce™ BCA Protein Assay Kit (Life Technologies, 23227). The RIPA-soluble fractions (25 µg total protein) were separated using NuPAGE Novex 4–12% Bis-Tris Gels (Invitrogen, NP0321) in NuPAGE MOPS SDS running buffer (Invitrogen, NP0001).

Proteins were transferred onto an Immobilon PVDF membrane (Merck, IPFL00010). Importantly, for the detection of CTFs, the membranes were boiled for 10 min in PBS, which enhanced the signal and reduced non-specific binding. Membranes were then blocked for 1 h in 5% dehydrated milk in PBST (1× PBS, 0.1% Tween-20; Sigma-Aldrich, P2287) before incubation with primary antibody (rabbit anti-TMEM106B, VIB_SB0051, 1:100; mouse anti-TMEM106B, Proteintech, 6033-1-Ig, 1:1000; rabbit anti-TMEM106B, Cell signaling, E7H7Z, 1:1000; rabbit anti-GAPDH, GeneTex, GTX100118, 1:20 000). Blots were then incubated with HRP-conjugated secondary antibodies and detected by enhanced chemiluminescence (Perkin-Elmer, NEL103001EA). For full-length TMEM106B protein, band intensities were quantified using ImageJ (NIH) and levels were normalized to GAPDH. On all blots, a linker sample was loaded twice, allowing data from multiple blots to be combined for analyses.

Immunoblot scoring

To determine the amount of TMEM106B CTF in the sarkosyl-insoluble fraction (P3), we used a semi-quantitative scoring system [0, no detectable band (no CTF); 1, faint band (mild CTF); 2, moderate band (moderate CTF); 3, prominent band (abundant CTF); 4, very prominent band (severe CTF)] (Supplementary Fig. 1). All cases were run twice on independent blots (replicates) and scored blinded by two researchers with an interrater reliability of 95.45%. When scores were discrepant between researchers, a final score was determined by consensus. For cases with a single point difference between replicates, the higher score was used as the final consensus score. For comparison of our immunoblot data with IHC, we also generated a simplified three-category scoring system including no/mild CTF burden (original immunoblot scores of 0 or 1), moderate CTF burden (original immunoblot scores of 2), and abundant/severe CTF burden (original immunoblot scores of 3 or 4), to allow more clearly delineated groups, with minimal bias introduced by the scoring used in the individual techniques.

Immunohistochemistry analyses

Immunostaining

Immunohistochemistry was performed on 4-µm thick sections of formalin-fixed, paraffin-embedded frontal cortex tissue, using a DAKO automated immunostainer (VIB_SB0051; 1:200). To improve

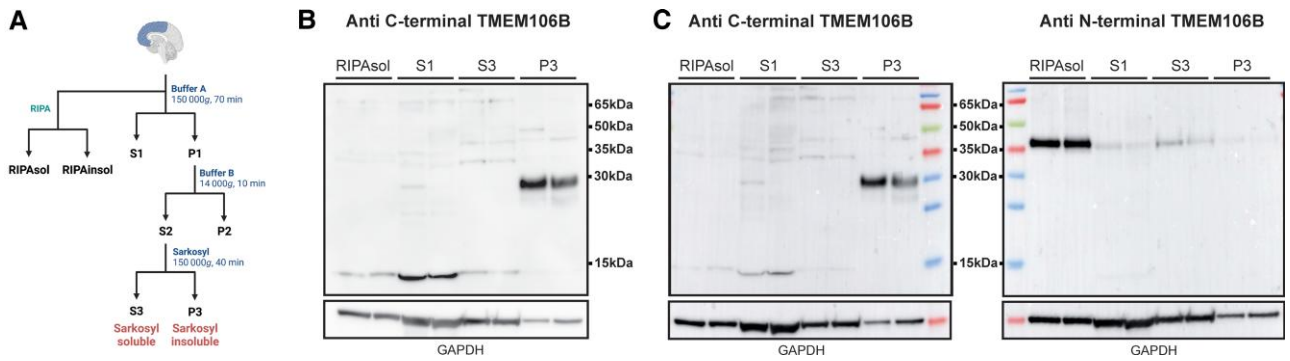

Figure 1 Fractionation protocol and antibody characterization. (**A**) Overview of protein fractionation protocol. (**B**) Immunoblot on the different protein fractions with the VIB_SB0051 antibody using blotting conditions optimized for the detection of TMEM106B CTF (~30 kDa) and (**C**) using blotting conditions optimized for the detection of full-length TMEM106B (~43 kDa) with VIB_SB0051 (*left*) or anti N-terminal TMEM106B (*right*) antibodies. The *bottom panel* shows GAPDH in each fraction. Ordered, from *left* to *right*, are three soluble fractions (RIPA, S1 and S3) and the sarkosyl-insoluble P3 fraction, each with two lanes representing two different cases. TMEM106B CTFs are only detected in the P3 fraction with the anti C-terminal antibody (VIB_SB0051), regardless of the conditions used. A band at ~43 kDa consistent with full-length TMEM106B is detected in all fractions with the anti N-terminal TMEM106B antibody but not with the anti C-terminal antibody (VIB_SB0051). Panel **A** was created with BioRender.

the staining quality, sections underwent manual pretreatment with formic acid (immersion in 98% FA for 6 min) as well as standard machine heat-retrieval (98°C for 30 min).

Immunohistochemistry scoring

All cases used in this study were part of a prior pathology study,[27] where a semi-quantitative pathology score was used (0, none; 1, mild; 2, moderate; 3, abundant; 4, severe). To compare the IHC with immunoblot data obtained in the current study, we similarly generated a simplified IHC scoring system with only three severity categories: no/mild pathology (original IHC scores of 0 or 1), moderate pathology (original IHC scores of 2) and abundant/severe pathology (original IHC scores of 3 or 4). For representative images of the modified IHC scores, see Supplementary Fig. 2A.

Antibody validation by immunoblot and immunohistochemistry

We confirmed the specificity of the VIB_SB0051 antibody by performing immunoblot analysis and IHC on frontal cortex tissue samples from cases in which the presence or absence of TMEM106B fibrils had previously been determined by cryo-EM.[1]

Data analysis

Statistical analyses were performed using IBM SPSS Statistics (version 28) and GraphPad Prism 9 (GraphPad Software, San Diego, CA). To determine differences in age between *TMEM106B* haplotype groups and pathology groups, a one-way ANOVA followed by Bonferroni's multiple comparisons *post hoc* test, was performed. To evaluate the correlation between immunoblot and IHC scoring, as well as with several parameters, a Spearman correlation analysis was performed. To account for covariates within the correlation (age, sex, *TMEM106B* haplotype), we performed a partial Spearman correlation analysis. Association between immunoblot score or IHC score and *TMEM106B* haplotype was further evaluated using a Kruskal–Wallis with Bonferroni *post hoc* test or Chi-square test with Bonferroni *post hoc* test. CTF burden scores were used as an ordinal variable. *P*-values <0.05 were considered statistically significant. Data are presented as mean ± SEM.

Data availability

The data associated with the analyses performed in this article are available as Supplementary Table 1.

Results

The VIB_SB0051 antibody recognizes insoluble TMEM106B CTF but not full-length TMEM106B

To confirm the specificity of the VIB_SB0051 antibody, we performed immunoblot analysis and IHC on eight cases previously analysed by cryo-EM.[1] On immunoblot, using the same experimental conditions as previously described for the detection of TMEM106B CTFs by Schweighauser *et al.*,[4] we detected a ~30 kDa band in the sarkosyl-insoluble fraction, corresponding to the expected size of the *N*-glycosylated TMEM106B CTF (Supplementary Fig. 2B). The six cases previously found to be positive by cryo-EM showed clear bands on immunoblot, whereas no bands were observed for a cryo-EM negative case (Case 60). Case 27, reported to have a limited number of high-quality fibrils, insufficient to generate a high-resolution cryo-EM map,[4] stained negative on immunoblot. IHC staining also matched the immunoblot and cryo-EM results, further verifying the specificity of our antibody (Supplementary Fig. 2C).

To further investigate the presence of TMEM106B CTFs across soluble and insoluble fractions we performed immunoblot analyses on both soluble (RIPAsol, S1 and S3) and insoluble (P3) protein fractions of frontal cortex brain tissue of two TMEM106B CTF positive cases (Fig. 1A). The ~30 kDa band was only present in the P3 sarkosyl-insoluble fraction and not in any of the soluble fractions (Fig. 1B). Furthermore, using this protocol, the antibody did not detect a band at the size corresponding to full-length TMEM106B. However, since we were aware that the detection of full-length TMEM106B protein is heat-sensitive, and our optimized protocol uses a longer boiling of the samples and boiling of the membrane in PBS prior to blocking, we separately performed immunoblotting with both the VIB_SB0051 as well as a commercially available anti N-terminal TMEM106B antibody, using conditions optimized to detect full-length TMEM106B protein. Full-length TMEM106B was detected in the RIPA-soluble (RIPAsol) and sarkosyl-soluble (S3) fractions and to a lesser extend in the S1 and P3 fractions using

the anti N-terminal antibody; however, even under these conditions, VIB_SB0051 still only detected a ~30 kDa band and did not demonstrate a band corresponding to full-length TMEM106B (Fig. 1C).

Insoluble TMEM106B CTFs are present in normal and diseased brain tissue

In the full cohort, 73% of samples ($n = 54$) showed an immunoreactive band at 30 kDa, with 52.7% ($n = 39$) classified as at least moderate (burden score ≥2). We detected insoluble TMEM106B CTF, with a range of different scores, in each of the different pathology groups and no significant differences were observed in frequency (Chi-square test, $P = 0.36$) or burden score (Kruskal–Wallis test, $P = 0.4$) of the bands among the major diagnostic groups (Fig. 2A). However, within the FTLD-TDP pathology group, we observed insoluble TMEM106B CTF in all *GRN* mutation carriers ($n = 10$) and all cases with sporadic FTLD-TDP type A ($n = 4$) (Fig. 2B). Six of seven cases which received the maximum immunoblot score of 4 were cases with TDP-43 pathology, of which four were *GRN* mutation carriers, one a sporadic FTLD-TDP type A case, and one a sporadic FTLD-TDP type C case. In fact, 70% of *GRN* mutation carriers had high amounts of insoluble TMEM106B (score ≥3) by immunoblot. Only one *GRN* mutation carrier had a mild insoluble TMEM106B CTF burden (score of 1); however, this case had the youngest age at death (49 years) and also carried a pathogenic *C9orf72* expansion. In neurologically normal individuals, 70% had no or very mild insoluble TMEM106B CTF burden, and the three individuals with scores of 2 or 3 were among the oldest in the group (71, 83, 99 years old).

Insoluble TMEM106B CTF burden correlates with age and *TMEM106B* haplotype

We found a significant association between age and *TMEM106B* CTF burden (ANOVA, $F = 7.05$, $P < 0.001$), with a significant difference between individuals having no fibrils and individuals with mild or abundant TMEM106B CTF burden in the insoluble fraction (Bonferroni *post hoc* test: 0–2, mean = –11.8 ± 3.83 years, $P < 0.05$; 0–3, mean = –17.8 ± 3.45 years, $P < 0.001$). Overall, we detected a positive correlation between age and immunoblot score ($r_s = 0.499$, $P < 0.001$) with virtually all individuals over the age of 65 years (93.5%) having insoluble TMEM106B CTF, as opposed to only 39.3% of younger individuals (<65 years; $n = 28$) (Fig. 2A). Interestingly, 6 of 11 young individuals that showed insoluble TMEM106B were *GRN* mutation carriers (Fig. 2B).

Considering that we found variability in the amount of insoluble TMEM106B CTF in individuals above the age of 65 years, which could not be explained by disease status, we next evaluated the contribution of both the *GRN* rs5848 genotype and the *TMEM106B* haplotype to CTF burden. While we did not observe a significant association with the *GRN* risk allele (rs5848:T; $P = 0.45$), we did find a significant association (Kruskal–Wallis test, $H = 12.23$, $P = 0.002$) and correlation ($r_s = 0.408$, $P < 0.001$) between the number of *TMEM106B* risk haplotypes and the insoluble TMEM106B CTF burden score. In the overall cohort, individuals with two *TMEM106B* risk haplotypes had higher amounts of insoluble TMEM106B CTF, as compared to individuals with two protective *TMEM106B* haplotypes (Bonferroni *post hoc* test: SS-TT, $P = 0.002$; TS-TT, not significant; SS-TS, not significant). The effect of the haplotype was also reflected in the proportion of individuals with each CTF burden score, which was significantly different across haplotype groups (Chi-square test, $\chi^2 = 20.37$, $P = 0.009$) (Fig. 2C) and remained significant even when *GRN* mutation carriers were excluded (Chi-square test, $\chi^2 = 17{,}40$, $P = 0.026$) (Fig. 2D). As there were no significant differences in age amongst individuals grouped by *TMEM106B* haplotype (ANOVA, $P = 0.953$), we concluded that the observed haplotype effect is not driven by age. Furthermore, controlling for *TMEM106B* haplotype using a partial Spearman correlation analysis increased the correlation of CTF immunoblot score with age ($r_s = 0.539$, $P < 0.001$) and, conversely, controlling for age increased the correlation of CTF immunoblot score with haplotype ($r_s = 0.469$, $P < 0.001$).

The combined effects of age and haplotype were easily detectable by immunoblot, with most young non-*GRN* cases having no or mild CTF burden and elderly cases with two protective haplotypes showing distinctly less TMEM106B CTF in the insoluble fraction (representative blot of series of Alzheimer's disease cases in Fig. 2E). Moreover, immunoblot analysis of cerebellar tissue from a subset of cases showed very similar results to those obtained from frontal cortex of the same individuals, indicating that the correlations of insoluble TMEM106B CTFs with age and *TMEM106B* haplotypes are not brain region-specific (Fig. 2F).

To investigate whether the variation in immunoblot results among the *TMEM106B* haplotype subgroups was due to differences in the solubility patterns of the CTFs, we evaluated the presence of TMEM106B CTFs in all of the soluble fractions (S1 and S3) in addition to the sarkosyl insoluble P3 fraction, in a representative subset of cases that included all haplotype combinations ($n = 11$). None of the samples showed TMEM106B CTFs (~30 kDa) in S1 or S3 fractions, suggesting that the associations with the amount of insoluble TMEM106B haplotype could not be explained by an altered solubility profile of the TMEM106B CTFs under these conditions (Supplementary Fig. 3).

We next quantified full-length TMEM106B protein in the RIPA-soluble fraction from frontal cortex in all cases to determine the relationship between CTF burden and the amount of physiological full-length TMEM106B. We detected considerable variability in the amount of full-length TMEM106B among cases, with no significant association (ANOVA, $P = 0.15$) but a weak inverse correlation ($r_s = –0.262$, $P = 0.025$) between the amount of full-length TMEM106B and insoluble CTF burden scores (Supplementary Fig. 4A). There were no significant differences in the amount of full-length TMEM106B among haplotype groups (ANOVA, $P = 0.158$) and only a non-significant inverse correlation between the amount of full-length TMEM106B and age ($r_s = –0.202$; $P = 0.08$) (Supplementary Fig. 4B). Since we did not observe a clear increase in full-length TMEM106B in elderly individuals or risk haplotype carriers, these findings suggest that age and *TMEM106B* haplotype may directly modulate the processing or formation of insoluble CTFs via some mechanism other than protein overexpression.

Immunoblot and immunohistochemistry show differences in TMEM106B CTF burden

All samples used in this study overlap with a separate larger descriptive pathology study,[27] making it possible to directly compare IHC analyses with our immunoblot results. Using a simplified scoring system we found that although the IHC and immunoblot scores positively correlated ($r_s = 0.662$; $P < 0.001$), 37.8% (28/74) of individuals differed in their IHC and immunoblot categories (Supplementary Table 1). In all but one of the cases with discrepant scores, more CTFs were detected by IHC and a much higher proportion of cases had abundant/severe CTFs detected by IHC than by immunoblot (62.2% versus 35.1%, respectively) (Fig. 3A). Indeed, the Spearman

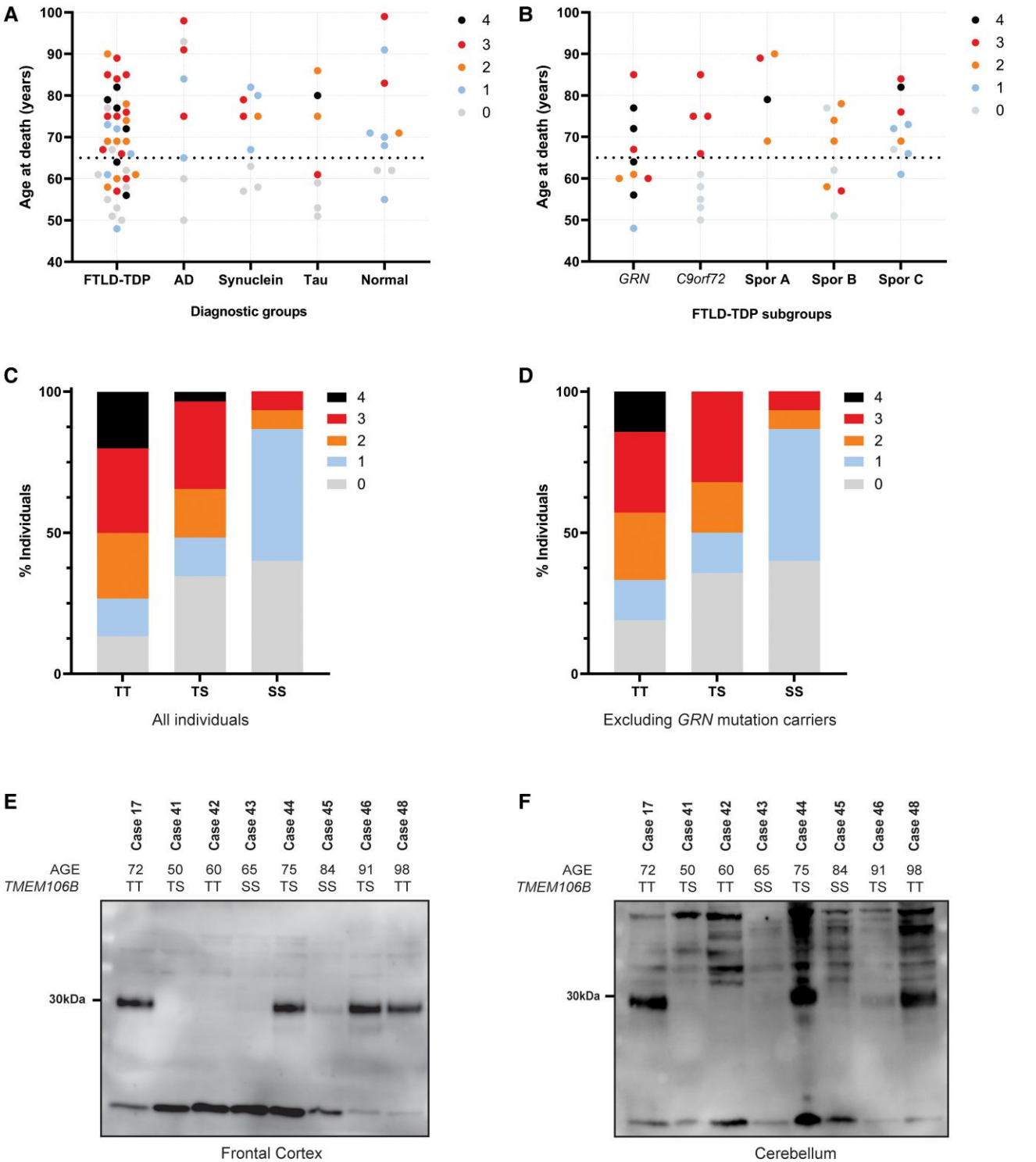

Figure 2 Burden of TMEM106B CTFs is associated with age and haplotype. (**A**) Age at death of all study cases in each major diagnostic group, with the colour of the dots representing the TMEM106B CTF burden score as measured by immunoblot. TMEM106B CTFs are present (immunoblot score of 1 or higher) in almost all individuals above 65 years (horizontal dotted line) regardless of diagnosis. Below 65 years of age, most individuals do not show CTFs by immunoblot (score of 0), except a number of FTLD-TDP cases. (**B**) Age at death of FTLD-TDP cases in each genetic/pathological subgroup, with the colour of the dots representing the TMEM106B CTF burden score as measured by immunoblot. TMEM106B CTFs are present in virtually all individuals over 65 years of age across all subgroups. Most younger individuals do not show CTFs by immunoblot, except for the *GRN* mutation carriers where at least some CTFs were present in all individuals regardless of age. (**C** and **D**) The proportion of individuals in each *TMEM106B* haplotype group with each TMEM106B CTF immunoblot score (indicated by colour), including (**C**) or excluding (**D**) *GRN* mutation carriers. (**E** and **F**) Representative immunoblots of sarkosyl-insoluble (P3) fraction from one *GRN* mutation carrier (Case 17; CTF positive control) and seven Alzheimer's disease (AD) cases, using the VIB_SB0051 antibody in samples of frontal cortex (**E**) and cerebellum (**F**). TMEM106B CTFs are only detected in AD cases with an age at death >65 years and the weakest signal was detected in Case 45, who carried the protective *TMEM106B* (SS) haplotype. *C9orf72* = *C9orf72* repeat expansion carriers; *GRN* = *GRN* mutation carriers; Spor A = sporadic FTLD-TDP type A; Spor B = sporadic FTLD-TDP type B; Spor C = sporadic FTLD-TDP type C; S = *TMEM106B* protective haplotype; T = *TMEM106B* risk haplotype.

correlation with age was stronger for IHC ($r_s = 0.7$, $P < 0.001$) than for immunoblot ($r_s = 0.5$, $P < 0.001$). While not significant, the mean ages in the different scoring categories also differed, with the mean age in the no/mild category for IHC being 57.16 ± 1.14 years as compared to 64.43 ± 1.96 years for immunoblot, and in the moderate category for IHC being 67.11 ± 1.56 years as compared to 71.92 ± 2.62 years for immunoblot. This suggests that although some individuals around the age of 65 years may still have no or mild insoluble TMEM106B CTF detectable by immunoblot, they may already have significant accumulation of CTF that can be demonstrated by IHC. This delay was especially apparent for the moderate IHC category where six of nine individuals showed either no or mild TMEM106B CTF burden in the insoluble fraction on immunoblot.

In addition to age, there were also clear differences in the association between TMEM106B CTFs and *TMEM106B* haplotype when comparing results from immunoblot and IHC (Table 1 and Fig. 3B–C). Using the three-category scoring system, immunoblot data showed a significant difference in distribution of *TMEM106B* haplotype carriers across CTF burden categories (Chi-square test, χ^2 = 14.56, $P = 0.006$), similar to what was observed with the five-category scoring system (Chi-square test, χ^2= 20.37, $P = 0.009$; Fig. 2C), and this difference remained significant even after exclusion of the *GRN* carriers (Chi-square test, χ^2= 10.25, $P = 0.036$) (Table 1). However, the IHC burden scores showed only a weak association with haplotype (Chi-square test, $\chi^2 = 9.97$, $P = 0.041$) that was lost when *GRN* mutation carriers were excluded (Chi-square test, $P = 0.252$) (Table 1). Differences between immunoblot and IHC results were also particularly noticeable in the group of neuropathologically normal individuals where all seven individuals above the age of 65 years were found to have moderate or abundant/severe pathology by IHC, but only three of these scored moderate or abundant/severe on immunoblot (aged 71, 83 and 99 years) (Fig. 3A, arrows). In conclusion, individuals with two protective *TMEM106B* haplotypes and neuropathologically normal individuals consistently showed lower CTF burden on immunoblot as compared to IHC.

Discussion

When genetic variants in and around *TMEM106B* were identified as the first known genetic risk factor for FTLD-TDP in 2010,[15] TMEM106B was a virtually unknown lysosomal protein with no prior link to neurodegenerative diseases or brain function. The strongest disease-modifying effect was observed in FTLD-TDP patients with *GRN* mutations, but in subsequent studies associations (albeit weaker) with common neurodegenerative diseases were also reported. For instance, *TMEM106B* variants were associated with both the risk to develop Alzheimer's disease and the pathological accumulation of TDP-43 inclusions in Alzheimer's disease brain, and the risk to develop cognitive decline in patients with Parkinson's disease and amyotrophic lateral sclerosis.[13,14]

Despite the clear biological impact of these *TMEM106B* variants, which are inherited together and collectively make up a *TMEM106B* haplotype, the functional variant(s) responsible for the reported associations remained elusive. In fact, research progress was somewhat hampered by the lack of antibodies recognizing the luminal TMEM106B C-terminus and the use of overexpression models to study possible functional variants.[7–12] Nevertheless, accumulating evidence is now pointing to two main mechanistic scenarios, which are not mutually exclusive: (i) *TMEM106B* haplotypes exert their effect by altering TMEM106B expression[24,25,28,29]; and/or (ii) there could be a functional effect of the coding p.T185S variant on TMEM106B biology or function.[30] Regardless of whether it is levels or the different TMEM106B protein isoforms, our view on TMEM106B biology has been transformed by recent cryo-EM studies which found amyloid-like fibrils composed of the CTF of TMEM106B (AA120–274) in brain tissue of a diverse set of neurodegenerative disorders and older neuropathologically normal individuals.[31] This discovery prompted us to study the abundance of these CTFs across a range of *TMEM106B*-associated diseases and determine their possible relationship to the disease-associated *TMEM106B* haplotype.

Using a novel antibody raised against recombinant AA239–250 peptide, located within the filament-forming core of TMEM106B, we observed a ~30 kDa band in the sarkosyl-insoluble fraction of post-mortem brain tissue, both in neuropathologically normal and diseased brain. The size corresponds to the predicted molecular weight of glycosylated TMEM106B CTF (120–254), consistent with what was observed by immunoblot by Schweighauser *et al.*,[4] using another antibody generated against the same TMEM106B C-terminal epitope. Importantly, the abundance of CTFs we detected by immunoblot closely correlated with cryo-EM findings previously generated on the same cases.[1] Also similar to the previous study,[4] our antibody did not detect full-length TMEM106B under the optimized conditions used in this study.

Given the strong genetic interaction between *TMEM106B* and FTLD-TDP, we predominantly focused our study on cases with different pathological and genetic subtypes of FTLD-TDP. However, since TMEM106B filaments were suggested to form in a non-specific age-dependent manner,[4] we also included cases with non-TDP-43 primary proteinopathies and neuropathologically normal individuals with a broad age range.

We detected TMEM106B CTFs in the sarkosyl-insoluble fraction of frontal cortex tissue in at least some individuals with each of the conditions and found that the formation of sarkosyl-insoluble TMEM106B CTFs is indeed an age-related feature across diagnostic groups, with the accumulation of CTFs in 93.5% of all patients above the age of 65 years. While this age cut-off is arbitrary, it appears to be in line with prior findings on the age-dependent genetic associations of *TMEM106B* with healthy ageing and suggest the insoluble fibrils may in fact contribute to these associations. Specifically, the effect of the *TMEM106B* risk variant on measures of biological ageing and on neuronal proportion was most prominent in individuals over 65 years.[22,23]

Interestingly, FTLD-TDP patients with *GRN* mutations were a clear exception, showing high amounts of insoluble TMEM106B CTFs in most patients, even at young age (<65 years). The consistent presence of extensive TMEM106B CTFs in these patients may be a result of the severe lysosomal dysfunction caused by the progranulin (PGRN) deficiency that results from all pathogenic *GRN* mutations. PGRN is cleaved within the lysosome into functional granulins which are critical for lysosomal function, and it has been shown that *in vitro* overexpression of TMEM106B severely reduces this cleavage event.[32,33] It is thus possible that the exceptionally strong modifying effect of the *TMEM106B* haplotype in *GRN* mutation carriers is due to increased levels of TMEM106B at the lysosomal membrane (associated with the risk haplotype), which further decreases granulin levels below a critical threshold (i.e. a double hit). In addition, the accumulation of aggregation-prone TMEM106B CTFs in the lysosome may further compromise lysosomal function.

In the other neurodegenerative disorders, the increase in TMEM106B CTFs with age may also result from lysosomal

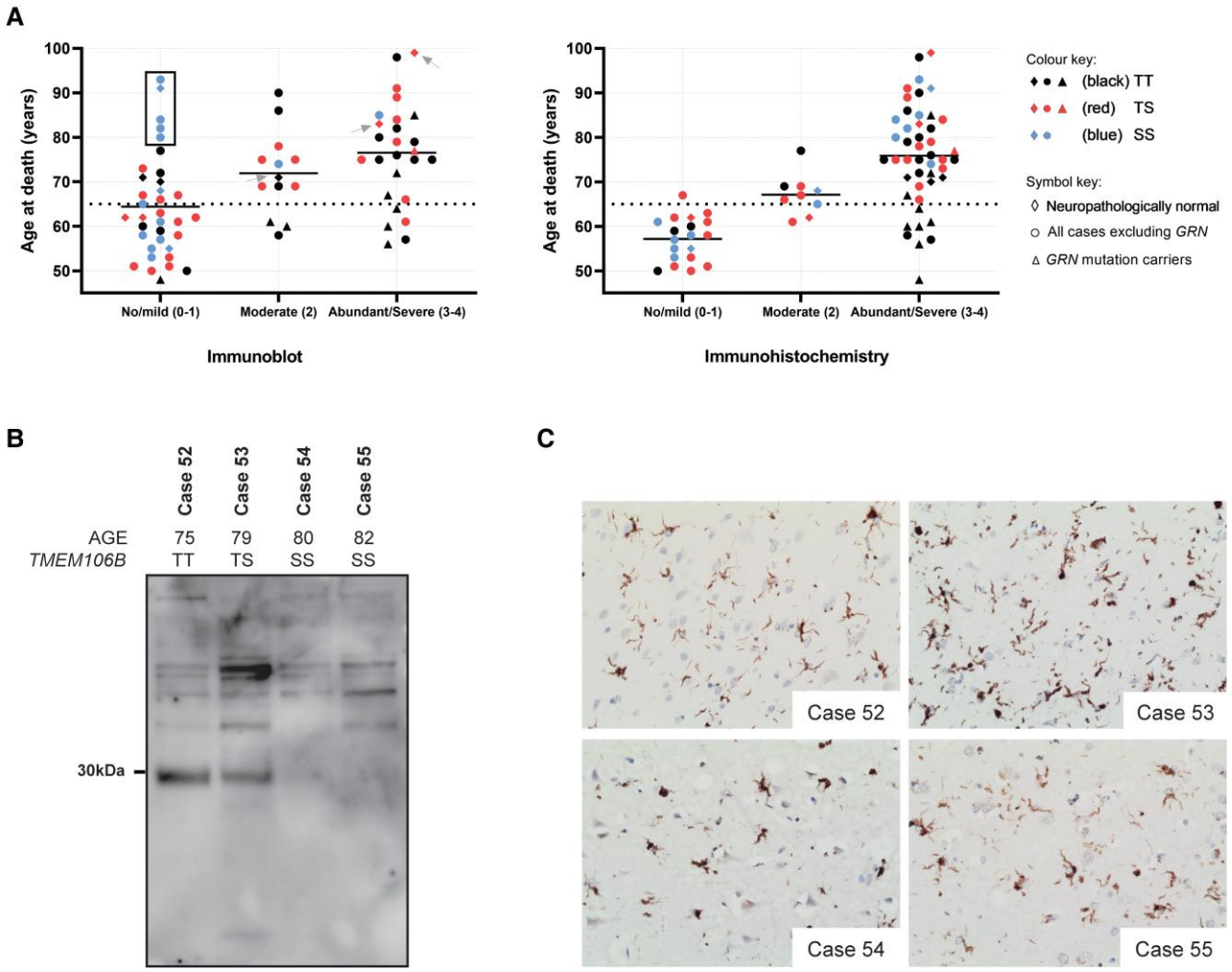

Figure 3 Age and haplotype correlation with TMEM106B CTF burden scores measured by immunoblotting and immunohistochemistry. (**A**) Age at death distribution of all study individuals, stratified by modified CTF burden score (no/mild, moderate or abundant/severe) measured by immunoblot (*left*) and immunohistochemistry (IHC) (*right*). Symbols represent different control and patient groups: diamonds are neuropathologically normal individuals, triangles are *GRN* mutation carriers and round dots indicate all other patient groups included in the study. The colour of the symbols indicates the *TMEM106B* haplotype. Horizontal dotted lines are used to indicate an age at death of 65 years, whereas full lines in each category represent the mean age at death in that group. Overall, more CTFs were detected by IHC than by immunoblot, with a larger proportion of cases presenting with abundant/severe IHC pathology as compared to immunoblot. Of note, the elderly individuals with two protective *TMEM106B* haplotypes (SS; highlighted by the black box) and neuropathologically normal individuals (diamond symbols), consistently showed a lower CTF burden on immunoblot as compared to IHC. In fact, of the 10 neurologically normal cases (diamonds) only the three oldest (grey arrows) had immunoblot scores greater than one. In addition, *GRN* mutation carriers (triangle symbols) had overall a higher burden of CTFs across both methods even in younger individuals, with all cases having abundant/severe pathology by IHC. (**B** and **C**) Immunoblot (**B**) and IHC (**C**) results of four representative Lewy-body disease cases above age at death of 65 years, carrying either two (Case 52), one (Case 53) or no (Cases 54 and 55) *TMEM106B* risk haplotypes (T). While immunoblot results show TMEM106B CTFs only in Cases 52 and 53, who carry at least one *TMEM106B* risk haplotype, IHC result shows TMEM106B pathology in all cases irrespective of *TMEM106B* haplotype.

dysfunction, e.g. secondary to the toxic accumulation of other disease proteins. However, once formed, TMEM106B fibrils could further promote or accelerate disease pathology and aggravate disease phenotype. More detailed correlation studies evaluating co-pathology or disease severity with the amount of insoluble TMEM106B CTFs will be necessary to provide further insights into this.

Excitingly, independent from the association with age, we found a highly significant association (Kruskal–Wallis test, $H = 12.23$, $P = 0.002$) and correlation ($r_s = 0.408$, $P < 0.001$) between TMEM106B CTFs and the disease-associated *TMEM106B* haplotypes, with higher amounts of insoluble TMEM106B CTFs in individuals carrying the risk haplotype. It is possible that the increased expression of *TMEM106B* that has previously been associated with the risk haplotype[24,25] results in elevated levels of physiological TMEM106B and the generation of more CTF and insoluble fibrils. However, our analyses of full-length RIPA-soluble TMEM106B did not demonstrate increased levels of full-length TMEM106B in risk haplotype carriers. This suggests a possible direct effect of the *TMEM106B* haplotypes on the cleavage of full-length TMEM106B or the formation of insoluble CTFs. For example, the protective p.T185S variant could induce differential processing of TMEM106B and/or changes in post-translational modifications, which could either directly modify the production of CTFs, or could affect the lysosomal localization of TMEM106B, in turn affecting the amount of TMEM106B available for cleavage in the lysosomes. Considering, a weak inverse

Table 1 Effect of *TMEM106B* haplotype on the distribution of cases across different CTF burden categories

–	No/mild	Moderate	Abundant/severe	*n*	P-value
Immunoblot					
Total cohort	35 (47.3%)	13 (17.6%)	26 (35.1%)	74	0.006
TT	8 (26.7%)	7 (23.3%)	15 (50%)[a]	30	
TS	14 (48.3%)	5 (17.2%)	10 (34.5%)	29	
SS	13 (86.7%)[a]	1 (6.7%)	1 (6.7%)	15	
Without *GRN*	34 (53.1%)	11 (17.2%)	19 (29.7%)	64	0.036
TT	7 (33.3%)	5 (23.8%)	9 (42.9%)	21	
TS	14 (50%)	5 (17.9%)	9 (32.1%)	28	
SS	13 (86.7%)[a]	1 (6.7%)	1 (6.7%)	15	
Immunohistochemistry					
Total cohort	19 (25.7%)	9 (12.2%)	46 (62.2%)	74	0.041
TT	3 (10%)	2 (6.7%)	25 (83.3%)[a]	30	
TS	10 (34.5%)	5 (17.2%)	14 (48.3%)	29	
SS	6 (40%)	2 (13.3%)	7 (46.7%)	15	
Without *GRN*	19 (29.7%)	9 (14.1%)	36 (56.3%)	64	0.252
TT	3 (14.3%)	2 (9.5%)	16 (76.2%)	21	
TS	10 (35.7%)	5 (17.9%)	13 (46.4%)	28	
SS	6 (40%)	2 (13.3%)	7 (46.7%)	15	

Values are presented as *n* (%). SS = homozygous for *TMEM106B* protective haplotype; TS = heterozygous; TT = homozygous for *TMEM106B* risk haplotype. Chi-square test with Bonferroni *post hoc* test.
[a]P-value <0.05.

correlation was observed between TMEM106B CTF and RIPA levels, it is also possible that a significant portion of full-length TMEM106B may have already been cleaved, obscuring any increase in physiological TMEM106B levels present in risk haplotype carriers. As our measurements of full-length TMEM106B in RIPA were quite variable, more precise ELISA-based assays should be used in the future to study the relationship between full-length TMEM106B, CTFs, and disease haplotypes.

Intriguingly, using our immunoblot analyses we detected a much stronger association between CTF burden and *TMEM106B* haplotypes than what was observed in a recent pathology study which used IHC for quantification.[27] In a direct comparison of both methods using an overlapping cohort of 74 cases, the IHC and immunoblot scores were overall positively correlated (r_s = 0.662; $P < 0.001$); however, discrepant results were found, especially in elderly individuals with two protective *TMEM106B* haplotypes. With IHC, many of these older *TMEM106B* SS cases showed abundant/severe TMEM106B CTF pathology, as would be expected based on age, but showed no or faint bands by immunoblot indicating no or mild CTF burden. While asymmetric anatomical distribution of pathological lesions may have influenced our findings (in cases where one hemisphere was used for IHC and another for immunoblot), the discrepancies were only found within specific phenotypic and genotypic groups with consistently more pathology on IHC as compared to immunoblot. What is the significance of this consistent discrepancy between IHC and immunoblot results in protective haplotype carriers, especially considering the strong disease associations of these haplotypes? Cryo-EM studies previously confirmed that individuals homozygous for the *TMEM106B* protective haplotype are capable of forming fibrils and even in our immunoblot analyses there was a single case (Case 9) with the 'SS' haplotype with abundant TMEM106B CTFs. Although the cryo-EM studies did find subtle differences in the structure of the filaments obtained from individuals who were homozygous for the protective haplotype, the number of these cases was insufficient to draw conclusions.[1–4]

It is tempting to speculate that the TMEM106B CTFs we observe by immunoblot are in fact toxic or otherwise contribute to the disease pathology across a range of different conditions; whereas the material detected by IHC includes additional CTFs that do not have these same characteristics and that are the predominant biochemical species in individuals homozygous for the *TMEM106B* protective haplotypes. This would be compatible with the fact that elderly (>65 years) neuropathologically normal individuals, who are apparently spared from neurodegeneration, often have abundant IHC pathology but strikingly less CTFs by immunoblot. It suggests that at least some of the TMEM106B staining observed by IHC may be the result of TMEM106B in a different stage of aggregation and solubility. While we were unable to detect the presence of any CTFs in the sarkosyl-soluble S1 and S3 fractions of the cases we analysed (which included some protective haplotype carriers), the amount of TMEM106B in these fractions may have been under the detection limit. It is also possible that changes in aggregation or assembly of TMEM106B CTFs or altered proteolytic processing of TMEM106B may occur based on the *TMEM106B* haplotype, all of which could result in an altered sensitivity of the antibody in different techniques.

To conclude, we show that the formation of sarkosyl-insoluble TMEM106B CTFs is an age-related feature that is clearly modified by *TMEM106B* haplotype, potentially underlying its disease-modifying effect. Furthermore, based on the comparative study of TMEM106B CTF burden using IHC and immunoblot analyses, we suggest that at least some insoluble TMEM106B CTFs may have a functional impact on brain health. However, untangling the pathogenicity of TMEM106B CTFs from the lysosomal dysfunction that is intrinsically associated with its formation will be challenging. Future detailed studies focusing on the structure and burden of filaments in cases with risk and protective *TMEM106B* haplotypes using different detection methods may hold the key to a better understanding of TMEM106B and its processing, and the development of disease-modifying treatment options.

Funding

This work was funded by grants from the University of Antwerp Research Funds (BOF), Vlaams Instituut voor Biotechnologie (VIB), and the National Institutes of Health (UG3 NS103870) (RR); the

Canadian Institutes of Health Research (74580) and the National Institutes of Health (U19AG063911) (IRAM). J.P. is supported by a fellowship from Research Foundation—Flanders (FWO). J.F. is supported by a Holloway Postdoctoral fellowship from the Association for Frontotemporal Degeneration (AFTD).

Competing interests

R.R. is a member of the Scientific Advisory Board of Arkuda Therapeutics and receives invention royalties from a patent related to progranulin. I.R.A.M. is a member of the Scientific Advisory Board of Prevail Therapeutics and receives invention royalties from a patent related to progranulin.

Supplementary material

Supplementary material is available at *Brain* online.

References

1. Chang A, Xiang X, Wang J, *et al*. Homotypic fibrillization of TMEM106B across diverse neurodegenerative diseases. *Cell*. 2022;185:1346-1355.e15.
2. Fan Y, Zhao Q, Xia W, *et al*. Generic amyloid fibrillation of TMEM106B in patient with Parkinson's disease dementia and normal elders. *Cell Res*. 2022;32:585-588.
3. Jiang YX, Cao Q, Sawaya MR, *et al*. Amyloid fibrils in FTLD-TDP are composed of TMEM106B and not TDP-43. *Nature*. 2022;605:304-309.
4. Schweighauser M, Arseni D, Bacioglu M, *et al*. Age-dependent formation of TMEM106B amyloid filaments in human brains. *Nature*. 2022;605:310-314.
5. Chiti F, Dobson CM. Protein misfolding, amyloid formation, and human disease: A summary of progress over the last decade. *Annu Rev Biochem*. 2017;86:27-68.
6. Sweeney P, Park H, Baumann M, *et al*. Protein misfolding in neurodegenerative diseases: implications and strategies. *Transl Neurodegener*. 2017;6:6.
7. Brady OA, Zheng Y, Murphy K, Huang M, Hu F. The frontotemporal lobar degeneration risk factor, TMEM106B, regulates lysosomal morphology and function. *Hum Mol Genet*. 2013;22:685-695.
8. Stagi M, Klein ZA, Gould TJ, Bewersdorf J, Strittmatter SM. Lysosome size, motility and stress response regulated by fronto-temporal dementia modifier TMEM106B. *Mol Cell Neurosci*. 2014;61:226-240.
9. Kundu ST, Grzeskowiak CL, Fradette JJ, *et al*. TMEM106B drives lung cancer metastasis by inducing TFEB-dependent lysosome synthesis and secretion of cathepsins. *Nat Commun*. 2018;9:2371.
10. Lüningschrör P, Werner G, Stroobants S, *et al*. The FTLD risk factor TMEM106B regulates the transport of lysosomes at the axon initial segment of motoneurons. *Cell Rep*. 2020;30:3506-3519.e6.
11. Lang CM, Fellerer K, Schwenk BM, *et al*. Membrane orientation and subcellular localization of transmembrane protein 106B (TMEM106B), a major risk factor for frontotemporal lobar degeneration. *J Biol Chem*. 2012;287:19355-19365.
12. Brady OA, Zhou X, Hu F. Regulated intramembrane proteolysis of the frontotemporal lobar degeneration risk factor, TMEM106B, by signal peptide peptidase-like 2a (SPPL2a). *J Biol Chem*. 2014;289:19670-19680.
13. Nicholson AM, Rademakers R. What we know about TMEM106B in neurodegeneration. *Acta Neuropathol*. 2016;132:639-651.
14. Feng T, Lacrampe A, Hu F. Physiological and pathological functions of TMEM106B: A gene associated with brain aging and multiple brain disorders. *Acta Neuropathol*. 2021;141:327-339.
15. van Deerlin VM, Sleiman PMA, Martinez-Lage M, *et al*. Common variants at 7p21 are associated with frontotemporal lobar degeneration with TDP-43 inclusions. *Nat Genet*. 2010;42:234-239.
16. Young JJ, Lavakumar M, Tampi D, Balachandran S, Tampi RR. Frontotemporal dementia: latest evidence and clinical implications. *Ther Adv Psychopharmacol*. 2018;8:33-48.
17. Olney N, Spina S, Miller BL. Frontotemporal dementia. *Neurol Clin*. 2017;35:339-374.
18. Liao YZ, Ma J, Dou JZ. The role of TDP-43 in neurodegenerative disease. *Mol Neurobiol*. 2022;59:4223-4241.
19. Mackenzie IRA, Neumann M, Baborie A, *et al*. A harmonized classification system for FTLD-TDP pathology. *Acta Neuropathol*. 2011;122:111-113.
20. van Blitterswijk M, Mullen B, Nicholson AM, *et al*. TMEM106B protects C9ORF72 expansion carriers against frontotemporal dementia. *Acta Neuropathol*. 2014;127:397-406.
21. Gallagher MD, Suh E, Grossman M, *et al*. TMEM106B is a genetic modifier of frontotemporal lobar degeneration with C9orf72 hexanucleotide repeat expansions. *Acta Neuropathol*. 2014;127:407-418.
22. Rhinn H, Abeliovich A. Differential aging analysis in human cerebral cortex identifies variants in TMEM106B and GRN that regulate aging phenotypes. *Cell Syst*. 2017;4:404-415.e5.
23. Li Z, Farias FHG, Dube U, *et al*. The TMEM106B FTLD-protective variant, rs1990621, is also associated with increased neuronal proportion. *Acta Neuropathol*. 2020;139:45-61.
24. Gallagher MD, Posavi M, Huang P, *et al*. A dementia-associated risk variant near TMEM106B alters chromatin architecture and gene expression. *Am J Hum Genet*. 2017;101:643-663.
25. Nicholson AM, Finch NA, Wojtas A, *et al*. TMEM106B P.T185S regulates TMEM106B protein levels: implications for frontotemporal dementia. *J Neurochem*. 2013;126:781-791.
26. Montine TJ, Phelps CH, Beach TG, *et al*. National institute on aging-Alzheimer's association guidelines for the neuropathologic assessment of Alzheimer's disease: a practical approach. *Acta Neuropathol*. 2012;123:1-11.
27. Perneel J, Neumann M, Heeman B, *et al*. Accumulation of TMEM106B C-terminal fragments in neurodegenerative disease and aging. *Acta Neuropathol*. 2023;145:285-302.
28. Chen-Plotkin AS, Unger TL, Gallagher MD, *et al*. TMEM106B, the risk gene for frontotemporal dementia, is regulated by the microRNA-132/212 cluster and affects progranulin pathways. *J Neurosci*. 2012;32:11213-11227.
29. Busch JI, Martinez-Lage M, Ashbridge E, *et al*. Expression of TMEM106B, the frontotemporal lobar degeneration-associated protein, in normal and diseased human brain. *Acta Neuropathol Commun*. 2013;1:36.
30. Jun MH, Han JH, Lee YK, Jang DJ, Kaang BK, Lee JA. TMEM106B, a frontotemporal lobar dementia (FTLD) modifier, associates with FTD-3-linked CHMP2B, a complex of ESCRT-III. *Mol Brain*. 2015;8:85.
31. Perneel J, Rademakers R. Identification of TMEM106B amyloid fibrils provides an updated view of TMEM106B biology in health and disease. *Acta Neuropathol*. 2022;144:807-819.
32. Zhou X, Paushter DH, Feng T, Sun L, Reinheckel T, Hu F. Lysosomal processing of progranulin. *Mol Neurodegener*. 2017;12(1):62.
33. Holler CJ, Taylor G, Deng Q, Kukar T. Intracellular proteolysis of progranulin generates stable, lysosomal granulins that are haploinsufficient in patients with frontotemporal dementia caused by GRN mutations. *eNeuro*. 2017;4:ENEURO.0100-17.2017.